Inorg. Chem. **2007**, *46*, 6108–6119

Cubane Variations: Syntheses, Structures, and Magnetic Property Analyses of Lanthanide(III)–Copper(II) Architectures with Controlled Nuclearities‖

Christophe Aronica,[†] Guillaume Chastanet,[†] Guillaume Pilet,[†] Boris Le Guennic,[‡] Vincent Robert,[‡] Wolfgang Wernsdorfer,[§] and Dominique Luneau*,[†]

Laboratoire des Multimatériaux et Interfaces (UMR 5615), Campus de La Doua, Université Claude Bernard Lyon 1, 69622 Villeurbanne Cedex, France, Laboratoire de Chimie (UMR 5182), Ecole normale supérieure de Lyon, 46 allée d'Italie, 69364 Lyon Cedex 07, France, and Institut Néel (UPR2940), BP 166, 25 Avenue des Martyrs, 38042 Grenoble Cedex 9, France

Received April 4, 2007

Starting from a molecular cubane $[Cu_4L_4]$ (**1**, with LH_2 = 1,1,1-trifluoro-7-hydroxy-4-methyl-5-aza-hept-3-en-2-one), we successfully replaced one and then two copper(II) ions of the cubane core by lanthanide ions to elaborate new families of 3d–4f complexes. Here, we report the syntheses, crystal structures, magnetic properties, and theoretical description of the tetranuclear copper(II) complex $[Cu_4L_4]$ (**1**, **[Cu$_4$]**) together with original yttrium(III) and gadolinium(III) heterometallic derivatives: $[YCu_3L_3(hfac)_3]^-$ (**2**, **[YCu$_3$]**); $[GdCu_3L_3(hfac)_3]^-$ (**3**, **[GdCu$_3$]**); $[Y_3Cu_6L_6(OH)_6(MeOH)_6(H_2O)_6]^{3+}$ (**4**, **[Y$_3$Cu$_6$]**); $[Gd_3Cu_6L_6(OH)_6(MeOH)_6(H_2O)_6]^{3+}$ (**5**, **[Gd$_3$Cu$_6$]**). **1** crystallizes in the $P2_1/c$ monoclinic space group with a cubane-like structure and shows ferromagnetic behavior. **2** and **3** crystallize in the $P\bar{1}$ triclinic space group and exhibit also cubane-like structures in which one copper(II) ion of the cubane core is substituted by one lanthanide ion. The magneto–structural correlations carried out on the yttrium(III) derivative reveal a spin frustration between the copper(II) ions that is retained in the gadolinium(III) analog ($J \sim -30$ cm^{-1}). **4** and **5** crystallize in the $C2/c$ monoclinic space group and result from the condensation of three $\{Ln_2Cu_2\}$ cubane-like moieties giving rise to nonanuclear architectures. On the basis of the theoretical investigations, it is suggested that the electronic distribution on the yttrium(III) ion may influence the magnetic interaction between the copper(II) pairs. Indeed, the sign and magnitude of the Cu–Cu interaction extracted from **4** do not seem to be retained in **5**. Thus, the introduction of lanthanide ions is likely to influence the nature of the Cu–Cu magnetic interactions in addition to their magnetic contribution. This work should contribute to improve the SMM synthesis strategy on the basis of the association of 3d and 4f ions.

Introduction

Among the richness of coordination chemistry, polynuclear metal complexes have focused an intense interest due, to their potential involvement in biological systems or in molecular-based electronic. For example, some polynuclear metal complexes are good synthetic models for iron−sulfur proteins or photosystem II, mostly based on cubane-like architectures.[1] Some others have been shown to behave as single-molecule magnets (SMMs), which are molecular entities that can be magnetized and exhibit hysteresis loops reminiscent of magnets.[2] This ability has led to important breakthroughs in the study of nanosize magnetic systems and currently focus a considerable amount of work due to potential applications in information processing.[3] To be an

* To whom correspondence should be addressed. E-mail: luneau@univ-lyon1.fr.
[†] Université Claude Bernard Lyon 1.
[‡] Ecole normale supérieure de Lyon.
[§] Institut Néel.
‖ This article is dedicated to the memory of Liliane G. Hubert-Pfalzgraf.

(1) a) Berg, J. M.; Holm, R. H. In *Structures and Reactions of Iron-Sulfur Protein Clusters and Their Synthetic Analogs, Iron-Sulfur Proteins 4*; Spiro, T. G., Ed.; Wiley-Interscience: New York, 1982; p 1. (b) Venkateswara Rao, P.; Holm, R. H. *Chem. Rev.* **2004**, *104*, 527. (c) Yachandra, V. K.; Sauer, K.; Klein, M. P. *Chem. Rev.* **1996**, *96*, 2927.
(2) (a) Caneschi, A.; Gatteschi, D.; Sessoli, R.; Barra, A.-L.; Brunel, L. C.; Guillot, M. *J. Am. Chem. Soc.* **1991**, *113*, 5873. (b) Sessoli, R.; Gatteschi, D.; Caneschi, A.; Novak, M. A. *Nature* **1993**, *365*, 141. (c) Sessoli, R.; Tsai, H.-L.; Schake, A. R.; Wang, S.; Vincent, J. B.; Folting, K.; Gatteschi, D.; Christou, G.; Hendrickson, D. N. *J. Am. Chem. Soc.* **1993**, *115*, 1804.
(3) Ritter, S. K. *Chem. Eng. News* **2004**, *82*, 29−32.

10.1021/ic700645q CCC: $37.00 © 2007 American Chemical Society
Published on Web 06/29/2007

SMM, a molecule must have a high-spin ground state (S) associated with a strong uniaxial magnetic anisotropy ($D < 0$).[2,4−7] These requirements induce two orientations of the magnetization (up and down) well-separated in energy. This energy barrier can be thermally overcome leading to dynamic magnetization fluctuations. An SMM is then equivalent to a superparamagnetic nanoparticle, and the way the magnetization is retained in one direction depends on the energy barrier roughly given by $|D|S^2$. Therefore, the larger D and S, the higher the barrier and the longer the magnetization should be retained in one direction. However, this barrier can be shortcut by quantum tunneling of the magnetization (QTM),[5,6] which contributes to speed up the overall relaxation process. Practically, the thermal and QTM processes coexist, leading to an experimental effective barrier U_{eff}, extracted from an Arrhenius law: $\tau = \tau_0 \exp(U_{eff}/kT)$. One of the main goals of the current research is to obtain systems with long relaxation times τ which is a crucial point for information storage applications.[6]

Accordingly, most efforts devoted to the chemical design of SMMs concentrate on the synthesis of large clusters with both high spin and anisotropy.[7] In this regard metal complexes with cubane-like structures are interesting starting points to elaborate high-spin molecules as generally ferromagnetic exchange couplings and high-spin ground state can be anticipated. In that sense, cubane-like compounds have received a considerable attention for many decades.[8−11] Besides, the introduction of lanthanide ions looks very promising since they associate high coordination numbers with large spin values and most of them have strong Ising-type magnetic anisotropy due to their important spin−orbit coupling.[12] Illustrative of this, several lanthanide-containing complexes exhibiting SMM behavior have been recently reported.[13−15] Whereas some of them are based on the only lanthanide ion,[13] the combination of 4f and 3d transition metal ions has turned out to be most successful.[14−15] Indeed, the magnetic exchange interaction interplays between d and f ions, even if they are usually rather small, may contribute to increase the ground spin state as well as the overall anisotropy. For instance, the Gd−Cu, Dy−Cu, and Tb−Cu interactions are known to be generally ferromagnetic.[16]

Along this strategy and starting from a tetranuclear copper(II) complex [Cu_4] with a cubane-like structure, we synthesized original Ln−Cu architectures with controlled nuclearities. Our approach consisted to progressively replace the copper(II) ions of the cubane core by one and then two lanthanide(III) ions with the challenging goal of scaling-up the ground spin state as well as the anisotropy. One major concern along this work has been to better understand the effects on the magnetic behavior when introducing one or several lanthanide ions in the cluster. Along this approach, we built up two series of heterobimetallic Ln(III)−Cu(II) clusters with four [$LnCu_3$] and nine [Ln_3Cu_6] nuclearities. The synthesis methodology works with most lanthanide ions, and we recently reported on a [Dy_3Cu_6] cluster that behaves as an SMM with a strong coercive field.[15]

In this paper we report the syntheses, crystal structures, and magnetic studies of the tetranuclear copper(II) complex [Cu_4L_4] (**1**, **[Cu$_4$]**) together with the yttrium(III) and gadolinium(III) heterometallic derivatives: $[YCu_3L_3(hfac)_3]^-$ (**2**, **[YCu$_3$]**); $[GdCu_3L_3(hfac)_3]^-$ (**3**, **[GdCu$_3$]**); $[Y_3Cu_6L_6(OH)_6(MeOH)_6(H_2O)_6]^{3+}$ (**4**, **[Y$_3$Cu$_6$]**); $[Gd_3Cu_6L_6(OH)_6(MeOH)_6(H_2O)_6]^{3+}$ (**5**, **[Gd$_3$Cu$_6$]**). We did not expect any SMM behavior for those compounds, and their study should be understood as part of a more complete work that aims at understanding, step by step, the different magnetic contribu-

(4) (a) Gatteschi, D.; Sessoli, R. *Angew. Chem., Int. Ed.* **2003**, *42*, 268. (b) Wernsdorfer, W. *Adv. Chem. Phys.* **2001**, *118*, 99.

(5) (a) Gatteschi, D.; Caneschi, A.; Pardi, L.; Sessoli, R. *Science* **1994**, *165*, 1054. (b) Müller, A.; Peters, F.; Pope, M. T.; Gatteschi, D. *Chem. Rev.* **1998**, *98*, 239.

(6) (a) Chudnovsky, E. M. *Science* **1996**, *274*, 838. (b) Leuenberger, M. N.; Loss, D. *Nature* **2001**, *410*, 789. (c) Hill, S.; Edward, R. S.; Aliaga-Alcalde, N.; Christou, G. *Science* **2003**, *302*, 1015.

(7) (a) Tasiopoulos, A. J.; Vinslava, A.; Wernsdorfer, W.; Abboud, K. A.; Christou, G. *Angew. Chem., Int. Ed.* **2004**, *43*, 2117. (b) Ako, A. M.; Hewitt, I. J.; Mereacre, V.; Clérac, R.; Wernsdorfer, W.; Anson, C. E.; Powell, A. K. *Angew. Chem., Int. Ed.* **2006**, *45*, 4926.

(8) (a) Merz, L.; Haase, W. *Z. Naturforsch* **1976**, *31a*, 177. (b) Jones, W. J.; Gupta, S.; Theriot, L. J.; Helm, F. T.; Baker, W. A., Jr. *Inorg. Chem.* **1978**, *17*, 87. (d) Bertrand, J. A.; Ginsberg, A. P.; Kaplan, R. I.; Kirkwood, C. E.; Martin, R. L.; Sherwood, R. C. *Inorg. Chem.* **1971**, *10*, 240. (e) Oshio, H.; Saito, Y.; Ito, T. *Angew. Chem., Int. Ed.* **1997**, *36*, 2673.

(9) (a) Halcrow, M. A.; Huffman, J. C.; Christou, G. *Angew. Chem., Int. Ed.* **1995**, *34*, 889. (b) Oshio, H. Oshino, N.; Ito, T. *J. Am. Chem. Soc.* **2000**, *122*, 12602. (c) Shiga, T.; Oshio, H. *Sci. Tech. Adv. Mater.* **2005**, *6*, 565. (d) Oshio, H.; Hoshino, N.; Nakano, M. *J. Am. Chem. Soc*. **2004**, *126*, 8804. (e) Yang, E.-C.; Wernsdorfer, W.; Hill, S.; Edwards, R. S.; Nakano, M.; Maccagnano, S.; Zakharov, L. N.; Rheingold, A. L.; Christou, G.; Hendrickson, D. N. *Polyhedron* **2003**, *22*, 1717. (f) Oshio, H.; Nakano, M. *Chem.−Eur. J.* **2005**, *11*, 1702. (g) Yang, E.-C.; Wernsdorfer, W.; Zakharov, L. N.; Karaki, Y.; Yamaguchi, A.; Isidro, R. M.; Lu, G.-D.; Wilson, S. A.; Rheingold, A. L.; Ishimoto, H.; Hendrickson, D. N. *Inorg. Chem.* **2006**, *45*, 529. (h) Dimitrou, K.; Folting, K.; Streib, W. E.; Christou G. *J. Am. Chem. Soc.* **1993**, *115*, 6432.

(10) (a) Aubin, S. M. J.; Wemple, M. W.; Adams, D. M.; Tsai, H.-L.; Christou, G.; Hendrickson, D. N. *J. Am. Chem. Soc.* **1996**, *118*, 7746. (b) Oshio, H.; Nihei, M.; Koizumi, S.; Shiga, T.; Nojiri, H.; Nakano Shirakawa, N.; Akatsu, M. *J. Am. Chem. Soc.* **2005**, *118*, 4568.

(11) (a) Ruiz, E.; Rodriguez-Fortea, A.; Alemany, P.; Alvarez, S. *Polyhedron* **2001**, *20*, 1323. (b) Tercero, K.; Ruiz, E.; Alvarez, S.; Rodriguez-Fortea, A.; Alemany, P. *J. Mater. Chem.* **2006**, *16*, 2729.

(12) Carlin, R. L. *Magnetochemistry*; Springer-Verlag: Berlin, 1986.

(13) (a) Ishikawa, N.; Sugita, M.; Ishikawa, T.; Koshihara, S.-Y.; Kaizu, Y. *J. Am. Chem. Soc.* **2003**, *125*, 8694. (b) Ishikawa, N.; Sugita, M.; Wernsdorfer, W. *Angew. Chem., Int. Ed.* **2005**, *44*, 2931. (c) Ishikawa, N.; Sugita, M.; Ishikawa, T.; Koshihara, S.-Y.; Kaizu, Y. *J. Phys. Chem. B* **2004**, *108*, 11265. (d) Tang, J.; Hewitt, I.; Madhu, N. T.; Chastanet, G.; Wernsdorfer, W.; Anson, C. E.; Benelli, C.; Sessoli, R.; Powell, A. K. *Angew. Chem., Int. Ed.* **2006**, *45*, 1729.

(14) (a) Mishra, A.; Wernsdorfer, W.; Parsons, S.; Christou, G.; Brechin, E. K. *Chem. Commun.* **2005**, 2086. (b) Mishra, A.; Wernsdorfer, W.; Abboud, K. A.; Christou, G. *J. Am. Chem. Soc.* **2004**, *126*, 15648. (c) Zaleski, C. M.; Depperman, E. C.; Kampf, J. W.; Kirk, M. L.; Pecoraro, V. *Angew. Chem., Int. Ed.* **2004**, *43*, 3912. (d) Osa, S.; Kido, T.; Matsumoto, N.; Re, N.; Pochaba, A.; Mrozinski, J. *J. Am. Chem. Soc.* **2004**, *126*, 420. (e) Murugesu, M.; Mishra, A.; Wernsdorfer, W.; Abboud, K. A.; Christou, G. *Polyhedron* **2006**, *25*, 613. (f) Mori, F; Nyui, T.; Ishida, T.; Nogami, T.: Choi, K.-Y.; Nojiri, H. *J. Am. Chem. Soc.* **2006**, *128*, 1440. (g) Osa, S.; Kido, T.; Matsumoto, N.; Re, N.; Pochaba, A.; Mrozinski, J. *J. Am. Chem. Soc.* **2004**, *126*, 420. (h) Zaleski, C. M.; Depperman, E. C.; Kampf, J. W.; Kirk, M. L.; Pecoraro, V. *Inorg. Chem.* **2006**, *43*, 10022

(15) Aronica, C.; Pilet, G.; Chastanet, G.; Wernsdorfer, W.; Jacquot, J.-F.; Luneau, D. *Angew. Chem., Int. Ed.* **2006**, *45*, 4659.

(16) (a) Kahn, M. L.; Mathonière, C.; Kahn, O. *Inorg. Chem.* **1999**, *38*, 3692. (b) Benelli, C.; Gatteschi, D. *Chem. Rev.* **2002**, *102*, 2369. (c) Costes, J.-P.; Dahan, F.; Dupuis, A.; Laurent J.-P. *Chem.−Eur. J.* **1998**, *4*, 1616. (d) Sanz, J. L.; Ruiz, R.; Gleizes, A.; Lloret, F.; Faus, J.; Julve, M.; Borras-Almenar, J. J.; Journaux, Y. *Inorg. Chem.* **1996**, *35*, 7384.

Scheme 1. Schematic Drawing of the LH_2 Ligand

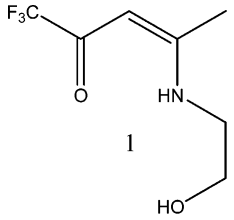

1

tions to the SMM behavior encountered in compounds such as $[Dy_3Cu_6]$.[15] Thus, the derivatives of the nonmagnetic yttrium(III) ion (**2** and **4)** were synthesized to get rid of the Cu−Ln magnetic interactions and to have some insight onto the only Cu−Cu interactions in these two series of mixed Cu(II)−Ln(III) systems. In compound **4** the role of Y(III) has been investigated by means of ab initio calculations. We then studied the gadolinium(III) derivatives in the light of the results obtained for the yttrium(III) analogs. The choice to synthesize the Gd(III) derivatives was motivated by the fact that this high-spin ion ($S = 7/2$) is magnetically isotropic. Thus, their study seems a prerequisite to the understanding of systems with anisotropic lanthanide ions such as $[Dy_3Cu_6]$ that shows an SMM behavior[15] but whose magnetic properties are much more complicated to understand.

Experimental Section

Syntheses. All chemicals and solvents were used as received; all preparations and manipulations were performed under aerobic conditions.

Ligand LH_2. The ligand 1,1,1-trifluoro-7-hydroxy-4-methyl-5-aza-hept-4-en-2-one results from the condensation of ethanolamine with the trifluoro-substituted acetylacetone (Scheme 1): 1 mL of ethanolamine (16.6 mmol; $M = 61.08$ g mol^{-1}; $d = 1.012$) was added to 2 mL of 1,1,1-trifluoro-2,4-pentanedione (16.5 mmol; $M = 154.09$ g mol^{-1}; $d = 1.27$) in 20 mL of methanol cooled in an ice bath. After the solution was stirred overnight, the methanol was removed under vacuum to give 2.1 g of a yellow solid further used without any purification ($M = 196$ g mol^{-1}; yield 65%).

$[Cu_4L_4]$ (1). The ligand LH_2 (0.2 g; 1.02 mmol) was dissolved in methanol (10 mL), and to this solution were added successively, under stirring, triethylamine (0.2 mL) and $CuCl_2{\cdot}4H_2O$ (0.17 g; 1 mmol; $M = 170.48$ g mol^{-1}). Slow evaporation of the resulting deep blue solution gave within 2 days 0.22 g of prismatic blue crystals of **1** which were isolated by filtration and washed with a small amount of methanol ($M = 1034.74$ g mol^{-1}; yield 85%). Anal. Calcd for **1** ($C_{28}H_{32}Cu_4F_{12}N_4O_8$): C, 32.49; H, 3.09; Cu, 24.58; F, 22.04; N, 5.41. Found: C, 32.43; H, 3.54; Cu, 24.79; F, 21.94; N, 5.34.

$(Et_3NH)[LnCu_3L_3Cl(hfac)_3]$ (with Ln = Y (2), Gd (3)). Both tetranuclear complexes were obtained by following the same procedure. The ligand LH_2 (0.2 g; 1.02 mmol) was dissolved in methanol (10 mL), and then 0.5 mmol of the lanthanide chloride in 10 mL of methanol was added dropwise ($YCl_3{\cdot}6H_2O$, 0.15 g, 0.50 mmol, $M = 303.36$ g mol^{-1}; $GdCl_3{\cdot}6H_2O$, 0.19 g, 0.51 mmol, $M = 371.7$ g mol^{-1}). The resulting light yellow solution was stirred for 30 mn. Then, 0.50 mmol of $CuCl_2{\cdot}2H_2O$ (85 mg; $M = 170.48$ g mol^{-1}) previously dissolved in 5 mL of methanol was added. It must be stressed here that the copper salt was added in default to prevent the formation of the very stable $[Cu_4L_4]$ cubane (**1**). To the resulting light green solution was added 0.2 mL of triethylamine leading to a deep blue solution. After being stirred for 30 min, the solution was concentrated under vacuum to a minimum of methanol. The possible presence of a nonsoluble species indicates the presence of the copper cubane $[Cu_4L_4]$ which has to be removed by filtration prior to proceeding. The concentrated solution was cooled in an ice bath, and then 0.2 mL of triethylamine and 0.5 mL of hexafluoroacetylacetone were added. After being stirred, the resulting solution turned clear green. The solvent was then slowly evaporated to give after 3 days green cubic shaped crystals of **2** and **3** suitable for single-crystal X-ray diffraction analyses. They were isolated by filtration and washed with a small amount of methanol leading to 178 mg of compound **2** (Ln = Y: $M = 1623.43$ g mol^{-1}; yield 47%) and 116 mg of compound **3** (Ln = Gd: $M = 1691.77$ g mol^{-1}; yield 29%). Anal. Calcd for **2** ($C_{42}H_{43}ClCu_3F_{27}N_4O_{12}Y$): C, 31.07; H, 2.65; Cl, 2.18; Cu, 11.74; Y, 5.48; F, 31.60; N, 3.45. Found: C, 31.36; H, 2.76; Cl, 2.32; Cu, 11.59; Y, 5.41; F, 31.53; N, 3.51. Calcd for **3** ($C_{42}H_{43}ClCu_3F_{27}N_4O_{12}Gd$): C, 29.82; H, 2.54; Cl, 2.10; Cu, 11.27; Gd, 9.29; F, 30.32; N, 3.31. Found: C, 29.85; H, 2.68; Cl, 2.34; Cu, 11.19; Gd, 9.27; F, 31.13; N, 3.39. **2** and **3** can also be obtained starting respectively from **4** and **5** by the addition of triethylamine and hexafluoroacetylacetone to their methanolic solutions.

$[Ln_3Cu_6L_6(OH)_6(MeOH)_6(H_2O)_6]Cl_3{\cdot}5H_2O$ (with Ln = Y (4), Gd (5)). Both nonanuclear complexes were obtained by following the same procedure as described hereafter. The ligand LH_2 (0.2 g; 1.02 mmol) was dissolved in methanol (10 mL), and 0.5 mmol of the lanthanide chloride in 10 mL of methanol was added dropwise. The resulting light yellow solution was stirred for 30 mn ($YCl_3{\cdot}6H_2O$, 0.15 g, 0.50 mmol, $M = 303.36$ g mol^{-1}; $GdCl_3{\cdot}6H_2O$, 0.19 g, 0.51 mmol, $M = 371.7$ g mol^{-1}). Then, 0.50 mmol of $CuCl_2{\cdot}2H_2O$ (85 mg; $M = 170.48$ g mol^{-1}) previously dissolved in methanol (5 mL) was added. As for **2** and **3** the copper salt was added in default to prevent formation of **1**. To the resulting light green solution was added 0.2 mL of triethylamine leading to a deep blue solution which gave after 1 week of slow evaporation square blue platelike crystals suitable for single-crystal X-ray diffraction analyzes. They were isolated by filtration and washed with a small amount of methanol to give 97 mg of **4** (Ln = Y: $M = 2448.77$ g mol^{-1}; yield 25%) and 112 mg of **5** (Ln = Gd: $M = 2653.8$ g mol^{-1}; yield 26%). Anal. Calcd for **4** ($C_{48}H_{100}Cl_3Cu_6F_{18}N_6O_{37}Y_3$): C, 23.52; H, 4.08; Cl, 4.34; Cu, 15.57; Y, 10.88; F, 13.97; N, 3.43. Found: C, 23.02; H, 3.87; Cl, 4.12; Cu, 16.12; Y, 11.05; F, 14.24; N, 3.71. Calcd for **5** ($C_{48}H_{100}Cl_3Cu_6F_{18}N_6O_{37}Gd_3$): C, 21.70; H, 3.38; Cl, 4.01; Cu, 14.37; Gd, 17.78; F, 12.89; N, 3.16. Found: C, 21.49; H, 3.36; Cl, 4.14; Cu, 14.57; Gd, 18.02; F, 13.34; N, 3.28.

Crystallography. Single-crystal X-ray studies of **1**−**5** were carried out using a Nonius KappaCCD and the related analysis software.[17] No absorption corrections were applied to the data sets. All structures were solved by direct methods using the SIR97 program[18] combined with Fourier difference syntheses and refined against F using reflections with $[I/\sigma(I) > 3]$ with the CRYSTALS program.[19] All atomic displacements parameters for non-hydrogen atoms have been refined with anisotropic terms. The hydrogen atoms were theoretically located on the basis of the conformation of the supporting atom.

Magnetic Measurements. Dc magnetic data were recorded using a Quantum Design SQUID magnetometer. The magnetic suscep-

(17) *NONIUS, Kappa CCD Program Package: COLLECT, DENZO, SCALEPACK, SORTAV*; Nonius BV: Delft, The Netherlands, 1999.
(18) Cascarano, G.; Altomare, A.; Giacovazzo, C.; Guagliardi, A.; Moliterni, A. G. G.; Siliqi, D.; Burla, M. C.; Polidori, G.; Camalli, M. *Acta Crystallogr., Sect. A* **1996**, *52*, C-79.
(19) Watkin, D. J.; Prout, C. K.; Carruthers, J. R.; Betteridge, P. W. *CRYSTALS Issue 11*; Chemical Crystallography Laboratory: Oxford, U.K., 1999.

tibilities were measured from 2 to 300 K on polycrystalline samples with applied field of 1 kOe. To avoid orientation in the magnetic field, the gadolinium samples were pressed in a home-made Teflon sample holder equipped with a piston. The magnetization was measured at 2 and 5 K in the 0−55 kOe range. The data were corrected for diamagnetism of the constituent atoms using Pascal's constants.

Micro-SQUID. Magnetization measurements on single crystals were also performed with an array of micro-SQUIDs.[4b] This magnetometer works in the temperature range ∼0.04−7 K with applied fields up to 140 kOe. The time resolution is approximately 1 ms. The field can be applied in any direction of the micro-SQUID plane with a precision smaller than 0.1° by separately driving three orthogonal coils. The field was then aligned to ensure the maximum signal. The thermalization is guaranteed by the fixation of the single crystals with Apiezon grease.

Computational Details. Explicitly correlated ab initio (configuration interactions, CI) and density functional theory (DFT) broken symmetry calculations have proven to be powerful tools in the understanding of magnetic systems. Nevertheless, we decided to perform CI calculations which use the exact Hamiltonian since the information extracted from a multiconfigurational wave function is very insightful into the mechanism of magnetic interactions. These calculations were performed on dimeric copper(II) units.

First, complete active space self-consistent field calculations (CASSCF) including 2 electrons in 2 molecular orbitals (CAS(2,2)) were performed using the MOLCAS package[20] to qualitatively incorporate the leading physical configurations. Along this multiconfigurational scheme, the contributions of the so-called ionic forms in the ground state singlet (2 e^- on one site) may be underestimated. Thus, one has to incorporate dynamical correlation effects to fully account for the singlet−triplet energy gap which defines the magnetic coupling constant *J*. Starting from the triplet molecular orbitals (MOs), dynamical correlation contributions were included using the difference dedicated configuration interaction (DDCI) method[21] implemented in the CASDI code.[22] This particular framework has shown to provide very accurate results for this type of compound and solid-state magnetic materials.[23] In the DDCI approach, one concentrates on the differential effects rather than on the absolute energies evaluation by assuming that the states of interest are described on a common set of MOs. In particular, all the double excitations from inactive MOs to virtual ones are not included in the CI space. The number of degrees of freedom (holes and particles) on top of the reference CASSCF wave function defines the successive DDCI-1, DDCI-2, and DDCI-3 levels of calculations. The physical contributions of the corresponding determinants have been debated in the literature.[24a,b] Along this procedure, we started with the triplet CASSCF MOs to build both states DDCI-1 density matrices. One can define average natural orbitals by diagonalizing the average density matrix. By the repetition of this operation, a common molecular basis set including spin-polarization effects was built along the IDDCI-1 scheme reported in the literature.[24,25] It has been shown that these crucial contributions are dominated by excitations involving the bridging-ligand orbitals. Finally, using these average DDCI-1 MOs, DDCI-2 and DDCI-3 simulations were performed over both states to grasp the relative importance of the different physical phenomena involved in the magnetic coupling. Extended atomic basis sets were used on dimeric units where the methyl and trifluoromethyl ligands were replaced by H atoms. A combination of (9s6p6d)/[3s3p4d] on the Cu atoms and (5s6p1d)/[2s2p1d] on the N, O, and sp^2 C atoms was used in our calculations.[26] Hydrogen and sp^3 carbon atoms were described with minimal STO-3G basis sets, i.e., (3s)/[1s] for H and (6s3p)/[2s1p] for C.[27] Finally, yttrium cations were included either as pure electrostatic point charges or together with a pseudopotential.[28] Let us stress that no basis set was included on the yttrium center. Nevertheless, we used the same MOs defined along the previous scheme in the absence of any yttrium ion. This procedure allows us to concentrate on the modifications of the wave function induced by the yttrium environment.

Results and Discussion

Syntheses. The choice of the ligand 1,1,1-trifluoro-7-hydroxy-4-methyl-5-aza-hept-4-en-2-one was made from a literature survey that shows that such ligand are known to give cubane-like clusters.[8] Moreover, this ligand has several donor sites which seem appropriate for the synthesis of heterometallic clusters. In this regard, there was in the literature a previous report of mixed Cu(II)−Ln(III) architectures using a similar ligand.[29] The reason to choose this ligand holding a CF_3 group (Scheme 1) was mainly that it facilitated the crystallizations of the compounds. Our similar attempts with the nonfluorinated analog have not been successful. Besides, we have also in mind that fluorinated ligands which are generally more volatile could be interesting when thinking to further applications such as in thin films processing.

With this ligand, we succeeded to synthesize, in a controllable way, two series of mixed tetranuclear [$LnCu_3$] and nonanuclear [Ln_3Cu_6] complexes containing copper(II) and lanthanide(III) ions. The tetranuclear complexes were synthesized with the help of an extra hfac ligand on the lanthanide ions. The nonanuclear cluster may be obtained also with chlorine anions or a mixture of chloride and perchlorate anions.[15] The synthesis processes work with most of the lanthanide ions (Y, Eu, Gd, Tb, Dy, Ho) and should be followed precisely as described in the Experimental Section. A crucial point is that the copper(II) ions should be kept in default (Cu(II)/ligand << 1) to avoid formation of the **[Cu_4]** cubane. In both tetranuclear and nonanuclear Ln(III)−Cu(II) series the basic framework of the clusters is a cubane core in which one or two of the copper(II) ions have been replaced by lanthanide ions. This holds for the tetranuclear complexes [$LnCu_3$] as well as for the nona-

(20) Anderson, K.; Fülscher, M. P.; Karlström, G.; Lindh, R.; Malqvist, P. A.; Olsen, J.; Roos, B.; Sadlej, A. J.; Blomberg, M. R. A.; Siegbahn, P. E. M.; Kello, V.; Noga, J.; Urban, M.; Widmark, P. O. *MOLCAS*, version 5.4; University of Lund: Lund, Sweden, 1998.
(21) Miralles, J.; Castell, O.; Caballol, R.; Malrieu, J. P. *Chem. Phys.* **1993**, *172*, 33.
(22) Ben Amor, N.; Maynau, D. *Chem. Phys. Lett.* **1998**, *286*, 211.
(23) Cabrero, J.; de Graaf, C.; Bordas, E.; Caballol, R.; Malrieu, J.-P. *Chem.−Eur. J.* **2003**, *9*, 2307.
(24) (a) Calzado, C. J.; Cabrero, J.; Malrieu, J. P.; Caballol, R. *J. Chem. Phys.* **2002**, *116*, 2728. (b) Calzado, J. C.; Cabrero, J.; Malrieu, J. P.; Caballol, R. *J. Chem. Phys.* **2002**, *116*, 3985. (c) de Loth, P. Cassoux, P.; Daudey, J. P.; Malrieu, J. P. *J. Am. Chem. Soc.* **1981**, *103*, 4007.
(25) Garcia, V. M; Castell, O.; Caballol, R.; Malrieu, J. P. *Chem. Phys. Lett.* **1995**, *238*, 22.
(26) Barandiaran, Z.; Seijo, L. *Can. J. Chem.* **1992**, *70*, 409.
(27) Hehre, W. J.; Stewart R. F.; Pople, J. A. *J. Chem. Phys.* **1969**, 2657.
(28) Abdalla, A.; Barandiaran, Z.; Seijo, L.; Lindh, R. *J. Chem. Phys.* **1998**, *108*, 2005.
(29) Benelli, C.; Caneschi, A.; Gatteschi, D.; Guillou, O.; Pardi, L. *Inorg. Chem.* **1990**, *29*, 1750.

Table 1. Crystal Data and Structure Refinement Parameters for Compounds **1**−**5**

param	[Cu_4] (**1**)	[Cu_3Y] (**2**)	[Cu_3Gd] (**3**)	[Cu_6Y_3] (**4**)	[Cu_6Gd_3] (**5**)
formula	$C_{28}H_{32}Cu_4F_{12}N_4O_8$	$C_{42}H_{43}Cl_1Cu_3F_{27}N_4O_{12}Y_1$	$C_{42}H_{43}Cl_1Cu_3F_{27}Gd_1N_4O_{12}$	$C_{44}H_{88}Cl_3Cu_6F_{18}N_6O_{33}Y_3$	$C_{46}H_{92}Cl_3Cu_6F_{18}Gd_3N_6O_{33}$
fw	1034.74	1623.77	1692.11	2325.52	2558.61
cryst syst	monoclinic	triclinic	triclinic	monoclinic	monoclinic
space group	$P2_1/c$ (No. 14)	$P\bar{1}$ (No. 2)	$P\bar{1}$ (No. 2)	$C2/c$ (No. 15)	$C2/c$ (No. 15)
a (Å)	13.8390(4)	13.0941(2)	13.0969(2)	29.000(2)	29.1239(9)
b (Å)	12.2627(4)	15.2755(2)	15.3158(3)	15.1494(8)	15.1022(4)
c (Å)	22.6302(5)	15.6275(2)	15.6664(3)	25.742(2)	25.8896(8)
α (deg)	90	78.095(1)	77.997(1)	90	90
β (deg)	96.785(2)	89.215(1)	89.331(1)	122.558(2)	123.054(1)
γ (deg)	90	82.666(1)	82.752(1)	90	90
V (Å^3)	3813.5(2)	3033.28(7)	3048.9(1)	9532(1)	9544.2(5)
Z	4	2	2	4	4
T (K)	293	150	150	150	150
λ(Mo Kα) (Å)	0.710 69	0.710 69	0.710 69	0.710 69	0.710 69
D (g·cm^{-3})	1.802	1.778	1.843	1.620	1.781
μ (mm^{-1})	2.310	2.168	2.288	3.302	3.551
$R(F)$,[a] $I > 3\sigma(F_o)$	0.0523	0.0452	0.0377	0.0641	0.0524
$R_w(F)$,[b] $I > 3\sigma(F_o)$	0.0614	0.0524	0.0452	0.0704	0.0598
S	1.10	1.10	1.08	1.10	1.07

[a] $R(F) = \sum||F_o| - |F_c||/\sum|F_o|$. [b] $R_w(F) = \sum[w((F_o^2 - F_c^2)^2/\sum wF_o^4]^{1/2}$.

nuclear complexes. Indeed, the latter family may be viewed as resulting from the fusion of three {Cu_2Ln_2} cubane cores sharing the lanthanide ions in a triangular fashion. Mixed-valence and heterometallic clusters with cubane-like frameworks have been already reported for 3d elements,[9−10] but to our best knowledge they are unprecedented for 3d−4f heterometallic systems related to the SMMs field. Among these compounds, some show SMM behavior as we have already reported in a previous article.[15]

Crystal and Molecular Structures. Compound **1** crystallizes in a monoclinic system, and according to the observed systematic extinctions, the structure was solved in the $P2_1/c$ space group. Compounds **2** and **3** crystallize in the triclinic system, and their structures were solved in the $P\bar{1}$ space group. Compounds **4** and **5** crystallize in a monoclinic system, and the structures were solved in the $C2/c$ space group. Table 1 summarizes the crystallographic data and refinement details for **1**−**5**. Selected bond lengths and angles are given in the Supporting Information (Tables S1−S5).

[Cu_4L_4] (1). The structure is very similar to those previously reported with the nonfluorinated ligand.[8a] The asymmetric unit is a neutral [Cu_4L_4] tetranuclear as the four ligands are fully deprotonated (L^{2-}) without any free solvent molecules (Figure 1). It consists of four alkoxo-bridged copper(II) ions, giving a slightly distorted cubic core {Cu_4O_4} of alternating copper and oxygen atoms. The pentacoordinated copper ions can be described as square pyramids, with the basal plane formed by one nitrogen and two oxygen atoms from one ligand and a third oxygen atom from another ligand. The apical position is occupied by an oxygen atom from a third ligand. The Cu−O and Cu−N bond lengths in the O_3N_1 square plane range from 1.890(5) to 1.962(4) Å (average: 1.935 Å) and from 1.930(5) to 1.948(6) Å (average: 1.937 Å), respectively. All distances are in good agreement with those previously reported for the nonfluorinated ligand (Table S1 in the Supporting Information).[8a] As it is usually observed, the oxygen atom coordinated in apical position exhibits a longer Cu−O bond length comprised between 2.400(4) and 2.451(4) Å (average: 2.420 Å). This copper(II) square pyramid environment is observed in all compounds **1**−**5** as described in the following. The cube belongs to the 4 + 2 class proposed by Ruiz et al.[11a] It is constituted of two types of planes. Four {Cu_2O_2} faces consist of two Cu−O−Cu angles (90 and 107°) and three short Cu−O distances (∼1.96 Å) and a longer one (2.42 Å). The last two {Cu_2O_2} faces differ by the presence of a unique Cu−O−Cu angle at 97° and two short (∼1.96 Å) and two long (∼2.42 Å) Cu−O distances.

(Et_3NH)[$LnCu_3L_3Cl(hfac)_3$] (with Ln = Y (2), Gd (3)). As both compounds are practically identical, differing only by the nature of the Ln(III) ion (Y (**2**) or Gd (**3**)), their crystal structures will be described simultaneously and referred to as [$LnCu_3$] (see Tables S2 and S3 in the Supporting Information). They consist of an anionic entity [$Ln_1Cu_3L_3(hfac)_3Cl$]$^-$ as all ligands L and hfac are fully deprotonated, without any free solvent molecules in the structure. The neutrality of the whole structure is assumed by one $(Et_3NH)^+$ cation (Figure 2a). The {$LnCu_3O_3Cl$} cubane core is built from three Cu(II) ions and one Ln(III) ion, the last four positions at the corners being occupied by one chlorine anion (μ_3-Cl^-) and three oxygen atoms (μ_3-O^-) coming from the three L^{2-} ligands (Figure 2b). The Ln(III) nine-coordinated sphere is constituted from three hfac ligands and three μ_3-O^- coming from three deprotonated ligands L^{2-}. The Ln(III)−O bond lengths (from 2.348(3) to 2.441(3) Å, average 2.395 Å in **2**; from 2.397(3) to 2.475(2) Å, average 2.429 Å in **3**) agree with those previously reported.[14−16] The five-coordinated Cu(II) ions are located in a square-base pyramid environment with the basal plane involving two oxygen and one nitrogen atoms from one ligand and a third oxygen atom from a second ligand. The apical position is occupied by the chlorine anion. The Cu−O bond lengths of the square planes range from 1.898(3) to 2.008(3) Å (average: 1.963 Å) in **2** and from 1.902(3) to 2.008(2) Å (average: 1.968 Å) in **3**. The Cu−N bond lengths are equal to 1.943(3) Å in **2** and are comprised between 1.939(3) and 1.951(3) Å (average: 1.945 Å) in **3**. The Cu−Cl bond lengths vary from 2.745(1) to 2.797(1) Å (average: 2.763 Å) and from 2.7458(9) to

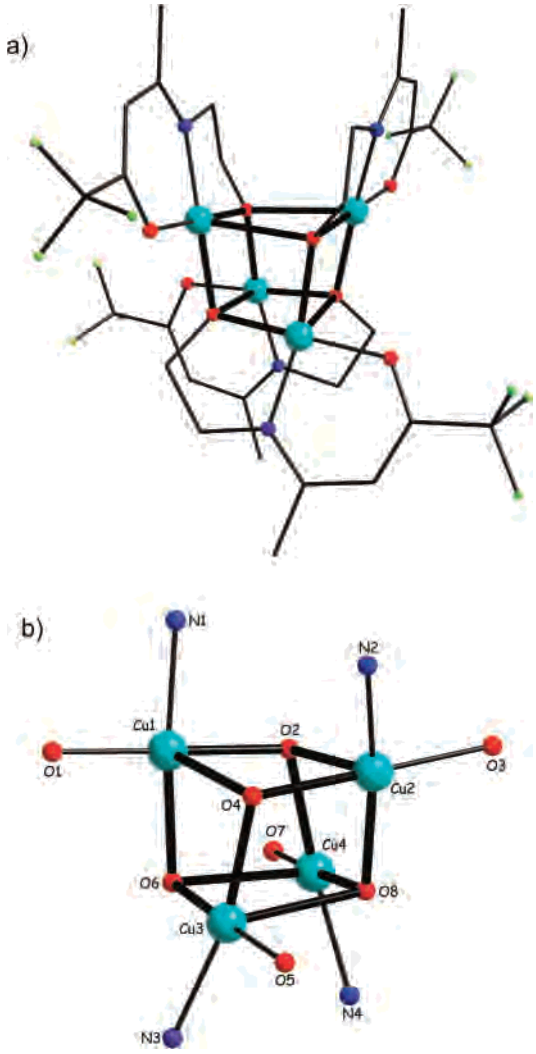

Figure 1. (a) Molecular structure of **1**. (b) View of the cubane core with labels used in the text.

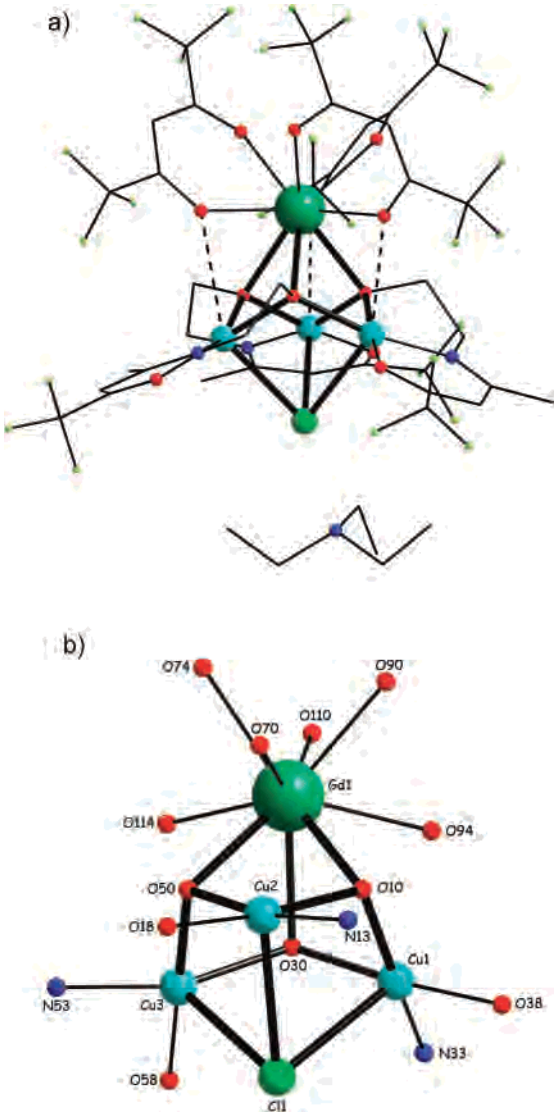

Figure 2. (a) Molecular structure of **2** similar to the structure of **3**. (b) View of the cubane core with labels used in the text.

2.7982(9) Å (average: 2.7634 Å) in **2** and **3**, respectively. In both compounds, the coordination sphere of the copper(II) ions is completed by one oxygen atom of a hfac ligand forming a distorted square-base bipyramidal environment. These three Cu···O distances are 2.613(3), 2.658(3), and 2.849(3) Å, respectively, in **2** and 2.654(2), 2.703(2), and 2.897(2) Å, respectively, in **3**. This illustrates the strong axial Jahn−Teller distortion as usually observed in copper(II) complexes.

Within the $\{LnCu_3O_3Cl\}$ cubane-like moieties, the bond angles strongly deviate from orthogonality due to the presence of a chlorine atom instead of an oxygen one. Indeed, the Cu−Cl−Cu angles vary from 74.32(3) to 76.29(3)° (average 75.4°) in **2** and from 74.33(2) to 76.31(2)° (average 75.4°) in **3**, whereas the Cu−O−Cu angles vary from 113.5(1) to 117.2(1)° (average 115.9°) in **2** and from 113.4(1) to 117.3(1)° (average 115.9°) in **3**. The Cu−O−Ln angles range from 97.4(1) to 100.2(1)° (average 98.6°) and from 97.13(9) to 100.32(9)° (average 98.6°) in **2** and **3**, respectively. Therefore, the $\{LnCu_3O_3Cl\}$ cubane core is highly distorted and can also be seen as a $\{LnCu_3Cl\}$ bipyramid with the triangular base formed by the three copper(II) ions (Figure 2b). This way, the oxygen atoms capped the three $\{LnCu_2\}$-faces. The averaged Cu−Cu and Cu−Ln distances equal respectively 3.381 and 3.361 Å in **2** and 3.382 and 3.393 Å in **3**. The anionic entities are well isolated from each other as we did not find any relevant hydrogen bonds between them.

$[Ln_3Cu_6L_6(OH)_6(MeOH)_6(H_2O)_6]Cl_3\cdot 5H_2O$ (with Ln = Y (4), Gd (5)). As both compounds differ only by the nature of the Ln(III) ion (Y (**4**) or Gd (**5**)), their crystal structures will be identically described and referred to as $[Ln_3Cu_6]$ (see Tables S4 and S5 in the Supporting Information). They consist of cationic entities $[Ln_3Cu_6L_6(\mu_3\text{-}OH)_6(\mu_1\text{-}H_2O)_{10}(MeOH)_6]^{3+}$ (Ln = Gd(III) or Y(III)) (Figure 3a) with three noncoordinated chlorine anions for the charge balance, as well as crystallization water molecules. The cationic entity is built from three Ln(III) ions arranged in a triangular way with $\{Cu_2L_2\}$ dimer units on each of the triangle edges (Figure 3b). Six alkoxo oxygen atoms of the deprotonated ligands (L^{2-}) and six OH^- groups bridge the different metal ions in a μ_3 way. The six OH^- groups connect the Ln(III)

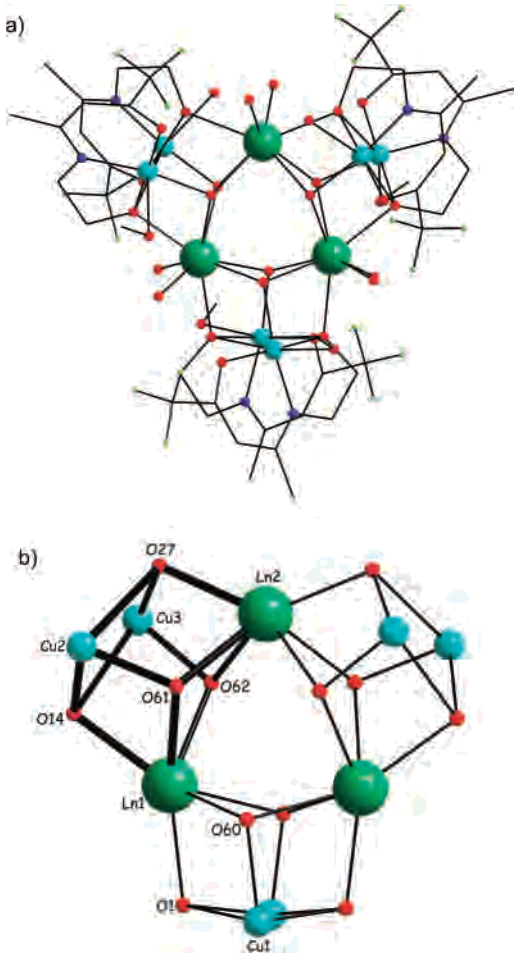

Figure 3. (a) Molecular structure of **4** similar to the structure of **5**. (b) View of the three $\{Ln_2Cu_2\}$ condensed cubane cores with the labels used in the text.

ions within the triangular framework $\{Ln_3(OH)_6\}$ and with the Cu(II) ions of adjacent $\{Cu_2L_2\}$ dimer units. One alkoxo bridge is used to connect the Cu(II) ions within the $\{Cu_2L_2\}$ dimer units and the second bridge with adjacent Ln(III) ions (Figure 3b). This results in distorted $\{Ln_2Cu_2L_2(OH)_2\}$ cubane-like moieties (Figure 3b) similar to homometallic cubane-like compounds.[8−9] The cationic entity may also be described as the condensation of three distorted $\{Ln_2Cu_2O_4\}$ cubane-like moieties sharing the Ln(III) ions in a triangular way. The structural features of the $\{Ln_2Cu_2L_2(OH)_2\}$ moieties are reminiscent of those reported for a $[Ln_2Cu_2]$ complex.[29] Within the $\{Ln_2Cu_2O_4\}$ cubane-like moieties, short and long Ln−Cu separations coexist. As in **2** and **3**, the cationic entities are well isolated from each other as we did not find any relevant hydrogen bonds in between.

The three Ln(III) ions exhibit the same eight-coordinated environment made by the oxygen atoms from two coordinated water molecules, four bridging OH^- groups, and two bridging alkoxo groups of the ligand (L^{2-}). The Ln(III)−O bond lengths (from 2.296(7) to 2.412(7) Å, average 2.364 Å in **4**; from 2.345(6) to 2.447(5) Å, average 2.364 Å in **5**) are in good agreement with the calculated ones.[10] Within the triangular framework $\{Ln_3(OH)_6\}$, the average Ln−Ln separations are equal to 3.791 and 3.848 Å for **4** and **5**, respectively. The Ln−O−Ln angles are almost identical (105°) whereas the Ln−O−Cu angles vary from 94.6(3) to 113.6(3)°. The six Cu(II) ions are basically five-coordinated in a square base pyramid with two oxygen and one nitrogen atoms from the ligand (L^{2-}) together with one OH^- group forming the basal plane. The fifth position is axially occupied by the alkoxo unit from the second ligand of the $\{Cu_2L_2\}$ dimer. The Cu−O bond lengths of the square planes range from 1.916(8) to 1.980(2) Å (average: 1.945 Å) in **4** and from 1.923(6) to 1.981(5) Å (average: 1.945 Å) in **5**. The Cu−N bond lengths are comprised between 1.92(1) and 2.006(2) Å (average: 1.957 Å) in **4** and between 1.935(7) and 1.946(7) Å (average: 1.942 Å) in **5**. The principal apical positions comprised between 2.553(9) and 2.652(8) Å (average: 2.618 Å) in **4** and between 2.573(7) and 2.658(7) Å (average: 2.617 Å) in **5** are located along Cu−O−Cu. A second axial position completes the five-coordination sphere of the copper(II) to six as one oxygen from the solvent molecules binds at 2.671(11), 2.765(11), and 2.920(8) Å, respectively, from the three dimers of **4** and at 2.697(9), 2.805(9), and 2.85(2) Å, respectively, from the three dimers of **5**. Within the three $\{Cu_2L_2\}$ dimer units, the Cu−O(alkoxo)−Cu bond angles are close to orthogonality (88.2 and 87.7° in **4** and **5**, respectively). The Cu−Cu separations are very similar in **4** and **5** (~3.18 Å).

Scheme 2. Schematic View of (a) **4** and (b) **5** Based on Structural Data with Exchange Interactions J_i

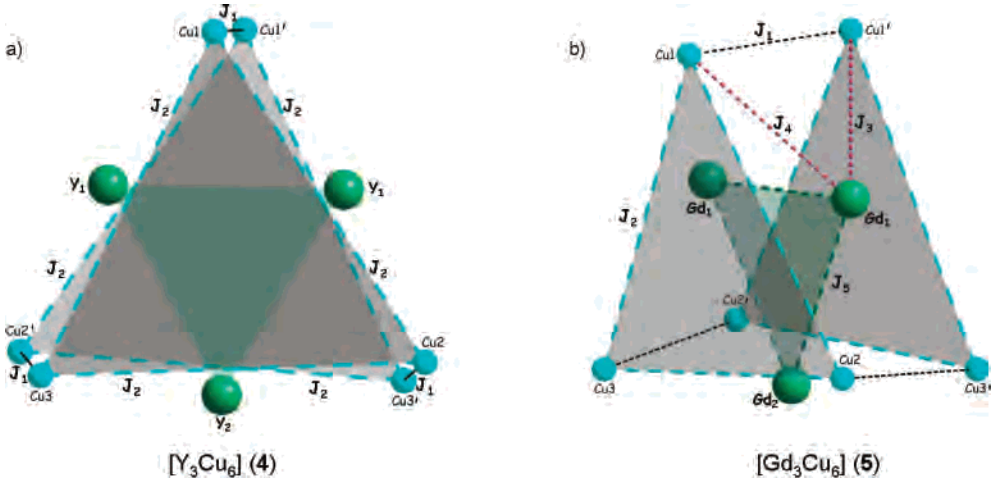

$[Y_3Cu_6]$ (**4**) $[Gd_3Cu_6]$ (**5**)

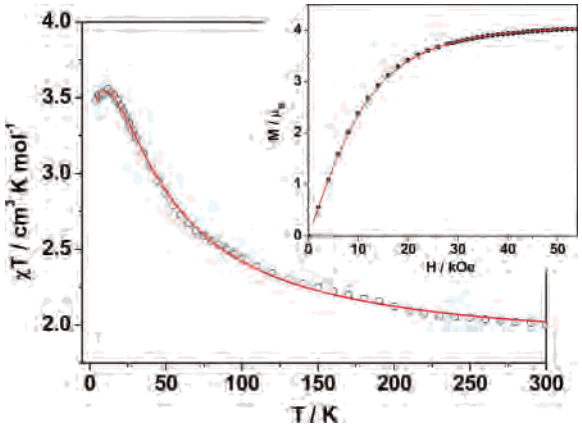

Figure 4. Temperature dependence of the χT product and magnetization at 2 K for **1**. The solid lines hold for the best fits of the data (see text).

The 3d−4f framework can be seen as three almost parallel and equilateral triangles. Both Cu_3 planes are tilted by 12° one to another, while the Ln_3 triangle lies in a staggered position (Scheme 2). The Cu−Cu separation within each triangle is 6.2 Å whereas the two Cu_3 triangles are separated by 3.2 Å. The corners of the triangles form copper(II) dimers. In the crystal packing the molecules are parallel one to another with a typical distance separation of 15−16 Å.

Magnetic Properties. The DC magnetic studies were carried out on polycrystalline samples of **1**−5 to obtain the thermal magnetic susceptibility (χ) behaviors and the isothermal magnetization data. Figures 4−8 display the thermal variation of the χT products and the magnetization curves for each compound.

[Cu_4] (1). The thermal variation of χT is shown in Figure 4. At room temperature, the χT product of 2.02 cm^3 K mol^{-1} is higher than the expected value for four Cu(II) ions considering a g value of 2.0 (1.5 cm^3 K mol^{-1}). Upon cooling, χT continuously increases and reaches a maximum of 3.55 cm^3 K mol^{-1} at 10 K close to the expected value for an $S = 2$ state. This feature indicates dominant intracluster ferromagnetic interactions. The decrease of the χT product below 10 K is ascribed to weak intermolecular antiferromagnetic interactions. The magnetization curve recorded at 2 K is reported in the insert of Figure 4. It shows a continuous increase up to the saturation value of 4.0 μ_B which corresponds well to a ground spin-state of 2, in agreement with the χT data.

This magnetic behavior, as well as the crystal structure, is very similar to those observed in the nonfluorinated analogue and other copper(II) cubanes.[8] Therefore, the data were analyzed using two different coupling constants J_1 and J_2, expressed in the spin Hamiltonian of eq 1 (Scheme 3), in agreement with the 4 + 2 class of cubane clusters.[11]

$$\hat{H} = -2J_1(\hat{S}_{Cu1}\hat{S}_{Cu4} + \hat{S}_{Cu1}\hat{S}_{Cu3} + \hat{S}_{Cu2}\hat{S}_{Cu4} + \hat{S}_{Cu2}\hat{S}_{Cu3}) - 2J_2(\hat{S}_{Cu1}\hat{S}_{Cu2} + \hat{S}_{Cu3}\hat{S}_{Cu4}) \quad (1)$$

In the analysis of the data, an intercluster interaction Θ was included as a mean field correction. The fit procedure leads to the following parameters: $g = 2.18$, $J_1 = +30.5$ cm^{-1}, $J_2 = -5.5$ cm^{-1}, and $\Theta = -0.10$ K (Figure 4). As may be expected, these values are close to those previously reported for the nonfluorinated analog.[8a] The magnetic behavior of such [Cu_4] systems has been explained elsewhere[8] and in a recent DFT study.[11] Shortly, the interactions between Cu1−Cu2 and Cu3−Cu4 involve two short [1.952(4)−1.959(5) Å] and two long [2.408(5)−2.456(5) Å] Cu−O bonds (Scheme 3). With this topology, the Jahn−Teller elongation within the copper pairs are directed in the Cu_2O_2 moieties (Cu1O4Cu2O2 and Cu3O6Cu4O8) so that the half-occupied $d_{x^2-y^2}$ orbitals are practically parallel to each other. Therefore, their overlap is rather small and results in the weak antiferomagnetic interaction (J_2).[11,30] In contrast, in the four other {Cu_2O_2} planes the $d_{x^2-y^2}$ orbitals of each copper(II) ions are nearly orthogonal which suppress the superexchange contribution and leads to the ferromagnetic interaction (J_1). The general ferromagnetic behavior is confirmed by the magnetic field dependence of the magnetization at 2 K. Indeed, the curve follows the Brillouin function for a ground spin-state $S = 2$, as expected for four Cu(II) ferromagnetically coupled, leading to a saturation value of 4 μ_B (insert of Figure 4).

Scheme 3. Drawing of the **[Cu_4]** Cubane Core with Exchange Couplings in Dashed Lines[a]

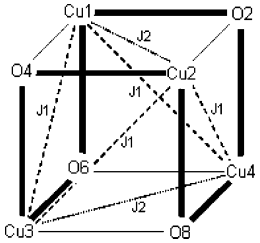

[a] The thick lines represent the short Cu−O bond lengths [1.952(4)−1.959(5) Å], while the thin lines represent the long ones [2.408(5)−2.456(5) Å].

[YCu_3] (2). The magnetic properties of compound **2** are reported in Figure 5a. At room temperature, the χT product is 1.25 cm^3 K mol^{-1}, which is close to the expected value for three uncoupled Cu(II) ions (1.125 cm^3 K mol^{-1}). Upon cooling, χT decreases and reaches a plateau below 30 K whose value (0.48 cm^3 K mol^{-1}) corresponds to an $S = 1/2$ spin state. This is confirmed by the field dependence of the magnetization at 2 K that reaches saturation at 1.11 μ_B corresponding to a doublet state (insert of Figure 5a).

Since the yttrium(III) ion is diamagnetic, it should not contribute to the magnetic behavior of **2**. Therefore, the magnetic data were analyzed on the basis of three copper(II) ions arranged in a triangle (Scheme 4a). According to the structural parameters, the copper triangle was considered equilateral and a single spin-coupling constant J_1 was taken into account to fit the magnetic behavior (eq 2).[31]

$$\hat{H} = -2J_1(\hat{S}_{Cu1}\hat{S}_{Cu2} + \hat{S}_{Cu1}\hat{S}_{Cu3} + \hat{S}_{Cu2}\hat{S}_{Cu3}) \quad (2)$$

(30) (a) Hatfield, W. E. *Comments Inorg. Chem*. **1981**, *1*, 105. (b) Kahn, O. *Inorg. Chim. Acta* **1982**, *62*, 3.
(31) (a) Ferrer, S.; Haasnoot, J. G.; Reedijk, J.; Müller, E.; Biagini Cingi, M.; Lanfranchi, M.; Manotti Lanfredi, A. M.; Ribas, J. *Inorg. Chem*. **2000**, *39*, 1859. (b) Kahn, O. *Chem. Phys. Lett.* **1997**, *265*, 109.

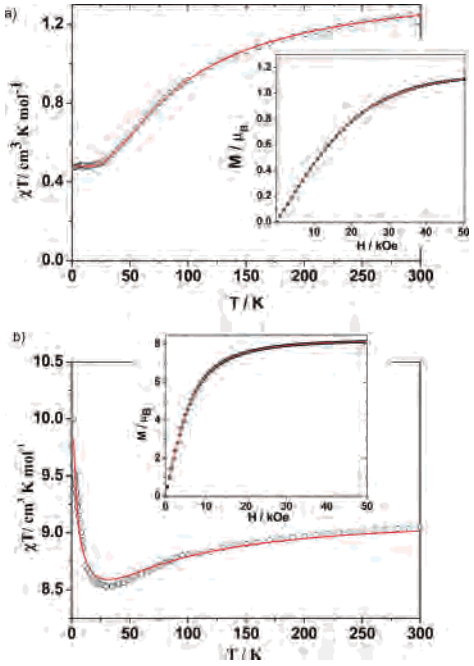

Figure 5. Temperature dependence of the χT product and magnetization at 2 K for (a) **2** and (b) **3**.

Scheme 4. Exchange Coupling in (a) **2** and (b) **3**

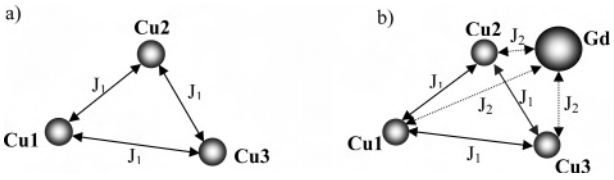

The fit of the χT curve leads to a g value of 2.26, J_1 of -28.2 cm^{-1}, and a small intermolecular interaction $\Theta = -0.013$ K (Figure 5a). Considering the system as isosceles did not improve the quality of the fit. The antiferromagnetic interaction between the copper(II) ions is coherent with the Cu−O−Cu and Cu−Cl−Cu bond angles of nearly 115 and 75°, respectively, which usually lead to antiparallel alignment of the spins.[30] Spin frustration between $S = {}^1/_2$ spin carriers is known to result in two degenerated doublet ground spin state which is in agreement with the χT value at low temperature and also with the fact that the magnetization curve at 2 K follows the Brillouin function for an $S = {}^1/_2$ ground spin state with an anisotropic g-value (insert of Figure 5a).

[GdCu$_3$] (3). The magnetic properties of compound **3** are reported in Figure 5b. The room-temperature χT value of 9.05 cm^3 K mol^{-1} nicely corresponds to the expected one for three Cu(II) and one Gd(III) ions ($S = 7/2$) (9 cm^3 K mol^{-1}). Upon cooling, χT continuously decreases to reach a minimum of 8.53 cm^3 K mol^{-1} at 30 K and then increases up to 10 cm^3 K mol^{-1} at 2 K. The magnetization at 2 K saturates at 8.14 μ_B indicating an $S = 4$ ground spin state. This is confirmed as the field dependence of the magnetization at 2 K follows the Brillouin function for an $S = 4$ spin (insert of Figure 5b).

As the gadolinium(III) ion is magnetic, the data analysis should now take into account the Gd−Cu exchange in addition to the Cu−Cu coupling (Scheme 4b). Thus, the spin Hamiltonian was written using two exchange coupling constants J_1 and J_2 for the Cu−Cu and Gd−Cu interactions, respectively:

$$\hat{H} = -2J_1(\hat{S}_{Cu1}\hat{S}_{Cu2} + \hat{S}_{Cu1}\hat{S}_{Cu3} + \hat{S}_{Cu2}\hat{S}_{Cu3}) - 2J_2(\hat{S}_{Gd}\hat{S}_{Cu1} + \hat{S}_{Gd}\hat{S}_{Cu2} + \hat{S}_{Gd}\hat{S}_{Cu3}) \quad (3)$$

The best fit of the χT curve was obtained with $g = 2.016$, $J_1 = -30.0$ cm^{-1}, $J_2 = +0.43$ cm^{-1}, and a small intermolecular interaction $\Theta = -0.03$ K (Figure 5b). Interestingly, the sign and amplitude of the antiferromagnetic interaction within the {Cu$_3$} moiety corresponds to those found in **3** as may be expected owing to the structural similarity of **2** and **3**. Also the weak ferromagnetic interaction between gadolinium(III) and copper(II) is in agreement with previously reported results.[16] This set of parameters is consistent with an $S = 4$ ground spin state resulting from the ferromagnetic coupling between the $S = 7/2$ of the gadolinium(III) ion and the $S = 1/2$ frustrated copper(II) triangle. This shows that the introduction of the Gd(III) ion in the cubane core increases successfully the spin of the ground state.

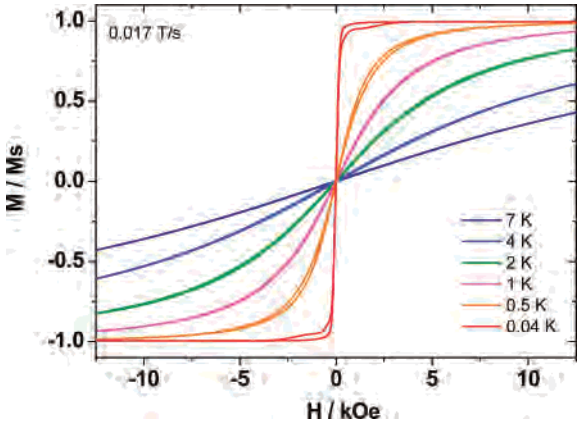

Figure 6. Magnetization curves for single crystals of **3** at various temperatures.

For comparison purpose with anisotropic systems, we investigated the thermal behavior of this "high-spin" cluster by measuring the magnetization on a single crystal of **3** at temperatures down to 40 mK and in fields up to 14 kOe using a micro-SQUID setup (Figure 6). As expected owing to isotropic character of the Gd(III) ion (4f^7), the low-temperature measurements for different directions of the applied field and the field sweep-rate studies did not show any significant hysteresis effect.

[Y$_3$Cu$_6$] (4). The magnetic properties of compound **4** are reported in Figure 7a. The room temperature χT value is 2.80 cm^3 K mol^{-1}, which is slightly higher than the expected value for six Cu(II) ions (2.25 cm^3 K mol^{-1}). Upon cooling, the χT value smoothly decreases down to 40 K and then drops abruptly down to 1.15 cm^3 K mol^{-1} at 2 K. The magnetization at 2 K does not fully saturate, even at 50 kOe where it reaches the value of 2.72 μ_B. This value is far from the 6 μ_B expected for six copper(II) ions.

At first glance, the copper ions framework in **4** may be viewed as made of three identical copper(II) pairs (Scheme

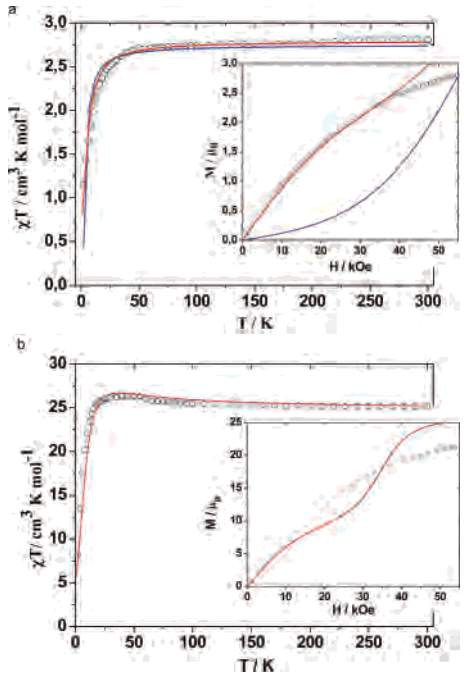

Figure 7. Temperature dependence of the χT product and magnetization at 2 K for (a) **4** and (b) **5**.

2a). Such a description leads to a simple dinuclear magnetic model taking into account a single exchange constant J_1 within the copper(II) pairs (Scheme 2a). Using this model, a very good fit of the χT curve was found with $g = 2.21$ and $J_1 = -2.16$ cm^{-1}. However, this model clearly failed to reproduce the magnetization curve (insert of Figure 7a, blue curve).[32] Thus, one has to think of a more sophisticated model involving additional magnetic interactions. In a first attempt we introduced a coupling constant between the $\{Cu_2\}$ pairs. However, this gave two antiferromagnetic constants that also failed to reproduce the magnetization curve. We then based our strategy on the triangular description of the clusters (Scheme 2). Accordingly a second coupling J_2 between the copper(II) of a triangle (Cu1−Cu2−Cu3 and Cu1′−Cu2′−Cu3′) was introduced in the model considering the following spin Hamiltonian:

$$\hat{H} = -2J_1(\hat{S}_{Cu1}\hat{S}_{Cu1'} + \hat{S}_{Cu2}\hat{S}_{Cu3'} + \hat{S}_{Cu3}\hat{S}_{Cu2'}) - 2J_2(\hat{S}_{Cu1}\hat{S}_{Cu2} + \hat{S}_{Cu2}\hat{S}_{Cu3} + \hat{S}_{Cu3}\hat{S}_{Cu1} + \hat{S}_{Cu1}\hat{S}_{Cu2'} + \hat{S}_{Cu2'}\hat{S}_{Cu3'} + \hat{S}_{Cu3'}\hat{S}_{Cu1'}) \quad (4)$$

On the basis of eq 4, a good fit of the χT curve was obtained with $g = 2.23$, $J_1 = 1.8$ cm^{-1}, and $J_2 = -2.2$ cm^{-1} (Figure 7a, red curves).[33] This result indicates a ferromagnetic coupling of the two triangles via their corners that is within the dimer moiety. The weakness of the antiferromagnetic interaction within the Cu_3 triangles (-2.2 cm^{-1}) is due to the long Cu−Cu distances (6.2 Å). The simulation of the magnetization curve with this set of parameters is better than the previous one.[32] However, above 25 kOe, the simulation strongly deviates from experiment (insert of Figure 7a). Introducing diagonal exchange interactions (Cu1−Cu3′, Cu1′− Cu2, ...) did not improve the simulation. Similar good simulation of the χT curve can be obtained with $g = 2.23$ and two antiferromagnetic interactions $J_1 = J_2 = -1.2$ cm^{-1}, but they give a poorer simulation of the magnetization curve.

Table 2. Magnetic Coupling Constant J_1 (cm^{-1}) from Calculations in Compound **4**

type	cation	J_1	complex	cation	J_1
CAS(2,2)[a]		−4.95	CAS(2,2)[c]	Y^{3+}	−0.46
CAS(2,2)[b]	Y^{3+}	1.04		Y^{2+}	−0.79
	Y^{2+}	−0.09			

[a] Yttrium cations are not included. [b] Yttrium cations are treated as a point charge. [c] Yttrium cations are included as an embedding ab initio model potential.

One can notice that in any case the set of interactions (J_1, J_2) are quite weak ($|J| \sim 2$ cm^{-1}). Moreover going from one model to the other completely changes the nature of the J_1 interaction within the $\{Cu_2\}$ moiety. From the structural point of view, the situation is not clear and the sign of this exchange interaction can hardly be predicted. Indeed, the Cu−O−Cu bond angles vary from 85.8 to 89.7°, which usually favor ferromagnetic couplings.[30] However the Cu_2O_2 planes in **4** and **5** are characterized by two long Cu−O distances due to the Jahn−Teller effect which increase the Cu−Cu interaction pathway and thus contribute to the weakness of the magnetic interaction.

To elucidate the nature (ferromagnetic vs antiferromagnetic) of the magnetic interaction in the copper(II) dimer moieties, Multi Reference Configuration Interactions (ab initio MRCI) calculations were performed. Even though the magnetic interactions are expected to be rather small, our goal was (i) to analyze the different contributions to the magnetic exchange and (ii) to investigate the role of the yttrium(III) ions on this exchange.

Let us first mention that at a CASSCF level with a CAS(2,2), the singlet and triplet are almost degenerate ($|J_1| <$ 0.1 cm^{-1}). The singlet wave function reads $\lambda|g\bar{g}| - \mu|u\bar{u}|$ with $\lambda \sim \mu$, reflecting the importance of correlation effects, g and u being the in-phase and the out-of-phase linear combinations of the $d_{x^2-y^2}$ Cu atomic orbitals. The magnetic orbitals resulting from the IDDCI-1 procedure are very similar to the CASSCF ones (Figure S1 in Supporting Information). Calculations with a larger active space (CAS(4,4)) including the in-phase and out-of-phase linear combination of p-type orbitals of the bridging oxygen atoms did not significantly modify the calculated J values. At this level of calculation, the singlet−triplet energy difference reveals an antiferromagnetic character ($J_1 \sim -5$ cm^{-1}). Nevertheless, one has to incorporate dynamical correlations effects to accurately order the singlet and triplet spin states. As seen in Table 2, these results are relatively sensitive to the environment of the magnetic ions. In particular, the inclusion of point charges +3 mimicking the yttrium(III) ions affects the magnetic interaction since the system switches from an antiferromagnetic to a ferromagnetic character. However,

(32) (a) Borras-Almenar, J. J.; Clemente-Juan, J. M.; Coronado, E.; Tsukerblat, B. S. *Inorg. Chem.* **1999**, *38*, 6081. (b) Borras-Almenar, J. J.; Clemente-Juan, J. M.; Coronado, E.; Tsukerblat, B. S. *J. Comput. Chem.* **2001**, *22*, 985.
(33) Gatteschi, D.; Pardi, L. *Gazz. Chim. Ital.* **1993**, *123*, 231.

antiferromagnetism is recovered as soon as the point charges are set to +2. Such description is known to be unsatisfactory, and a more realistic modelization includes pseudopotential on the yttrium ions. Using such a description, whatever the yttrium charge (Table 2), a weak antiferromagnetic character is obtained. Thus, one cannot rule out the participation of the yttrium(III) in the magnetic coupling mechanism. However, such detailed analysis is out of the scope of this paper as both experiments based on neutron diffraction and theoretical investigations would be required. We plan to investigate further this crucial issue. Indeed, it has already been reported that yttrium ions can hold a spin density which may affect the magnetic behavior.[34]

[Gd_3Cu_6] (5). The magnetic properties of compound **5** are reported in Figure 7b. At room temperature the χT product is 25.15 cm^3 K mol^{-1}, which is slightly lower than the expected value for six copper(II) ions and three gadolinium(III) (25.87 cm^3 K mol^{-1}). Upon cooling, the χT value smoothly increases to reach a maximum of 26.20 cm^3 K mol^{-1} at 35 K and then decreases rapidly to 8.27 cm^3 K mol^{-1} at 2 K. The magnetization data recorded at 2 K do not fully saturate, even above 50 kOe where the value reaches a value of 21.27 μ_B, lower than the expected 27 μ_B. Clearly, the ground-state spin value of the cluster is not easily determined.

Considering the difficulties we encountered in the magnetic description in **4**, the analysis of the magnetic behavior of **5** appeared hazardous. Indeed, there are at least five different coupling constants that should be taken into account (see Scheme 2b), i.e. two Cu−Cu (J_1 and J_2), two Cu−Gd (J_3 and J_4), and one Gd−Gd (J_5). Moreover, there are all expected to be quite weak. Indeed, we have seen from **4** that the Cu−Cu magnetic interaction should be weaker than 3 cm^{-1}, whatever the sign. The Cu−Gd coupling is also known to lead to weak ferromagnetic exchange[16] while the Gd−Gd exchange within the central triangle should be antiferromagnetic but weak (<-0.2 cm^{-1}) as suggested in a previous study of a similar trinuclear gadolinium(III) system.[35] At least one set of parameters can fit the χT curve ($g = 1.96$, $J_1 = -15$ cm^{-1}, $J_2 = -2.2$ cm^{-1}, $J_3 = 2.4$ cm^{-1}, $J_4 = 2.5$ cm^{-1}, $J_5 = -0.25$ cm^{-1}; see Figure 7b, red curves). However, as for **4** this set of parameters fails to accurately fit the magnetization behavior.

As for compound **[$GdCu_3$]** (**3**) and for comparison purpose with more anisotropic systems of the [Ln_3Cu_6] series, we performed μ-SQUID magnetization measurements on single-crystals of **[Gd_3Cu_6]** (**5**) at low temperatures (Figure 8). Even if the temperature effect is rather weak as the sharpness of the curves is not much affected and the remanence quite small, a narrow hysteresis with a coercive field of 200 Oe is observed at 0.2 K. Obviously, this gadolinium(III)-containing complex may not be considered as magnetically isotropic.

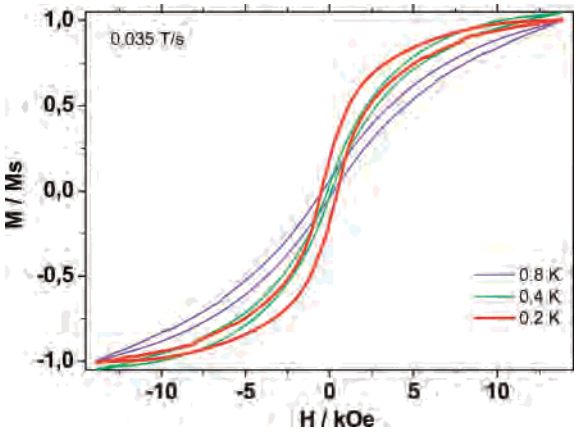

Figure 8. Magnetization curves for single crystals of **5** at different temperatures.

However, the origin of this small magnetic anisotropy is rather difficult to elucidate. It may come from the effect of the ligand field on the gadolinium(III) orbitals. One cannot also exclude the effect on the overall anisotropy of the magnetic interactions within {Gd_3} triangles and between Cu(II) and Gd(III). Indeed, such a behavior was not observed in **[$GdCu_3$]** (**3**). To clarify this particular issue we plan to perform polarized neutron diffraction on both yttrium and gadolinium derivatives to extract spin density maps.

Concluding Remarks

Starting from a cubane-like compound **[Cu_4]**, we succeeded in synthesizing in a controlled way two series of Ln(III)−Cu(II) clusters. They are made of cubane-like frameworks in which one or two copper(II) ions have been replaced by lanthanide ions. This is an important result that should be stressed here as one concern for the future of SMMs is the ability to design predictable polynuclear architectures.[36] While this synthetic approach of 3d−4f polynuclear systems strengthens the design of SMMs, it may be also relevant to other field such as the oxide precursors of the YBaCuO superconductor types, for example.[37]

In this paper we presented the results for the yttrium(III) and gadolinium(III) derivatives. The crystal structure of all compounds has been fully determined, and their magnetic behaviors have been characterized. Despite structural similarities, the Cu−Cu interactions range from −30 to +30 cm^{-1}, reflecting the strong sensitivity of the magnetic exchange coupling to the environment. In particular, the Cu−Cu magnetic interactions were shown to be influenced by the presence of lanthanide ions. Indeed, our calculations on the **[Y_3Cu_6]** cluster suggest that the yttrium(III) ion may not be innocent. This deserves further investigations that will combine theoretical calculations and experimental determination of the spin and charges densities.

In the light of our study, several points may be emphasized. (i) The origin of the small anisotropy revealed on

(34) (a) Claiser, N.; Souhassou, M.; Lecomte, C.; Gillon, B.; Carbonera, C.; Caneschi, A.; Dei, A.; Gatteschi, D.; Bencini, A.; Pontillon, Y.; Lelievre-Berna, E. *J. Phys. Chem. B* **2005**, *109*, 2723. (b) Pontillon, Y.; Bencini, A.; Caneschi, A.; Dei, A.; Gatteschi, D.; Gillon, B.; Sangregorio, C.; Stride, J.; Totti, F. *Angew. Chem., Int. Ed.* **2000**, *39*, 1786.
(35) Costes, J.-P. ; Dahan, F.; Nicodème, F. *Inorg. Chem.* **2001**, *40*, 5285.
(36) Winpenny, R. E. P. *Dalton Trans.* **2002**, 1−10.
(37) (a) Hubert-Pfalzgraf, L. G.; Guillon, H. *Appl. Organomet. Chem.* **1998**, *12*, 321. (b) Zhang, J.; Hubert-Pfalzgraf,L. G.; Luneau, D. *Inorg. Chem. Commun.* **2004**, *7*, 979. (c) Zhang, J.; Morlens, S.; Hubert-Pfalzgraf, L. G.; Luneau D. *Eur. J. Inorg. Chem.* **2005**, 3928.

[Gd_3Cu_6] by the hysteresis loops at low temperatures cannot be clearly identifed. Additional calculations have to be performed to clarify the effect of the coordination geometry of the gadolinium(III) ion; a detailed study of the [Gd_3][35] analog should give some outline on the influence of the antiferromagnetic exchange within the {Gd_3} triangle and therefore on the importance of the Cu−Gd interactions. (ii) These systems will be useful as references to discuss the magnetism of anisotropic systems such as [Dy_3Cu_6].[15] A confrontation between [Dy_3][13d] and [Dy_3Cu_6], which possess a similar {Dy_3} framework, indicates that the {Ln_3} triangles are sufficiently magnetoanisotropic on their own to generate SMM behavior. In our system the additional copper(II) ions seem to favor a nonzero ground spin state in contrast to the quasi-null ground spin state of [Dy_3]. However, one cannot currently estimate the importance of the non-colinearity of the J ($L+S$) vectors of the lanthanide(III) ions on the magnetoanisotropy of the clusters.

Even if several questions are still unsolved, the availability of these Ln−Cu systems as well as the previous reported [Ln_3] systems give us a chance to investigate in detail these factors. This should contribute to improve the SMM synthesis strategy on the basis of the association of 3d and 4f ions. Such a study will be extended to other 3d metal ions and other paramagnetic species such as the nitroxide free radicals which are interesting building blocks to design high-spin molecules.[38]

Acknowledgment. The "Région Rhône-Alpes" and the network of excellence MAGMANet are gratefully acknowledged for financial support. Funding and instrumental supports for magnetic measurements were provided by the "Commissariat à l'Energie Atomique" (CEA) through a "Laboratoire de Recherche Conventioné" (LRC No. DSM-03-31). Single-crystal X-ray diffraction studies were performed at the "Centre de Diffractometrie Henri Longchambon" at Université Claude Bernard Lyon 1. The French Ministry of Research and Education supported this work through a Ph.D. grant to C.A. G.C. is very grateful to Dr. Olivier Cador for fruitful discussions. B.L.G. and V.R. thank the Institut de Développement et de Ressources en Informatique Scientifique (IDRIS) for computing facilities.

Supporting Information Available: X-ray crystallographic file in CIF format for compounds **1**−**5** (**[Cu_4]**, **[Cu_3Y]**, **[Cu_3Gd]**, **[Cu_6Y_3]**, **[Cu_6Gd_3]**), selected interatomic distances and angles for compounds **1**−**5** (Tables S1−S5), and the scheme of the magnetic orbitals for copper(II) dimeric moieties obtained by ab initio calculations for **4**. This material is available free of charge via the Internet at http://pubs.acs.org.

IC700645Q

(38) (a) Luneau, D.; Rey, P. *Coord. Chem. Rev.* **2005**, *249*, 2591 and references therein. (b) Vostrikova, K. E.; Luneau, D.; Verdaguer, M.; Wernsdorfer, W.; Rey, P. *J. Am. Chem. Soc.* **2000**, *122*, 718.